Eur. Phys. J. B **26**, 35–39 (2002)
DOI: 10.1140/epjb/e20020063

**THE EUROPEAN PHYSICAL JOURNAL B**
EDP Sciences


# Correlation between compacity distributions in compressed Si powders and in Si sintered pellets

S. Dubois[a], E. Béré, P. Grosbras, and A. Straboni

Laboratoire de Métallurgie Physique[b], boulevard P. et M. Curie, bâtiment SP2MI, BP 30179, 86960 Futuroscope Cedex, France

Received 14 September 2001 and Received in final form 18 December 2001

**Abstract.** Resistivity measurements have been performed on silicon powder beds with different thicknesses which were submitted to uniaxial pressure (0–640 MPa). For the smallest thicknesses of the Si pellets, the pressure dependence of conductivity may be described using models based on effective medium theory or strongest stresses network. For largest Si thicknesses, it exists an inhomogeneous distribution of pressure in the granular medium as a consequence of arching effects. It is shown that the conductivity variation with Si powder thickness may be understood using a distribution of conductivity induced by the distribution of pressure. Finally, it is shown that the conductivity of the sintered Si pellets is correlated with the uniaxial compression step.

**PACS.** 45.70.Cc Static sandpiles; granular compaction – 72.80.Tm Composite materials

## 1 Introduction

Polycrystalline silicon materials have attracted a great deal of interest due to a lot of advantages for microelectronic, flat panel displays and photovoltaïc applications. Its conductivity level and type can be adjusted by conventional doping and the obtained conductivity values are very high due to the important carrier mobilities. Moreover its high stability allows for the use of high temperature treatments. The production of large and thick substrates in photovoltaïc applications is actually limited by the cost of material and wafer preparations. To overcome these limitations, a new method has recently been proposed to synthesize polycrystalline materials dedicated to photovoltac applications. It consists in sintering beds of silicon powder with thickness of a few hundreds of microns [1]. The main objective is turned towards a strong cost reduction of the material itself but also of the elaboration processes by enabling large area forming techniques. This technology includes an important step of compaction of the powder beds before sintering. This step is also of prime importance as the final compacity of the material is strongly dependent on the morphology resulting from the compacting procedure.

An external pressure is thus needed to both shape the powder and promote higher packing densities. The initial transition with pressurization is from a loose array of particles to a closer packing. The first response is rearrangement of the particles that leads to a higher contact density between grains. For most materials, the point contacts subsequently deform as the pressure increases, this step is known as the Hertz regime. The mechanical properties of random packing of cylinders having nearly the same diameter submitted to uniaxial compression have been studied together with their photoelastic properties [2,3]. The macroscopic response was shown to be strongly non linear and the relation between force and displacement ($\delta$) is being given by $F \propto \delta^m$. An exponent $m = 3.9$ was found, it is much larger than the expected value 1.5 for an individual Hertz contact. A numerical model of this problem has been studied by Stauffer *et al.* [4,5]. It consists in an array of parallel cylinders of slightly fluctuating radii submitted to an uniaxial compression. The power law regime is similar to the one observed by photoelastic study. The discrepancy between the value of the macroscopic exponent m and its value in the microscopic case for the deformation of two cylinders in contact is attributed to the local heterogeneities created by geometrical imperfections of the cylinders. Deviation to the Hertz law results from the radius fluctuations which induce an inhomogeneous repartition of the contacts between cylinders and of the intergranular stresses. Applied stress is transmitted *via* a network of stressed particles, also known as the strongest stresses network.

As expected from the mechanical properties, a nonlinear macroscopic response has also been observed for the dependence of conductivity with applied force [6]. For spheres or cylinders submitted to an uniaxial pressure, the macroscopic conductivity of the system, derived from Hertz microscopic law [7], is expected to vary as $\sigma \propto F^t$ where $t$, the microscopic exponent derived from Hertz law, equals 1/3. For instance, at low stress, grains rearrange by rotations and local slidings and Hertz deformations play

[a] e-mail: sylvain.dubois@univ-poitiers.fr
[b] UMR 6630

a little role. As a consequence, the power law is not valid. At intermediate stress, the strongest stresses network, as observed in mechanical behavior, has a lower electrical resistance than the overall real contacts between particles. As a consequence, current is mostly transmitted from the strongest stresses network. Upon increasing pressure, new strength lines are created on the strongest stresses network and contributes to an increase of the conductivity. A power law regime is observed in this range of forces but the exponent is larger than the microscopic exponent derived from Hertz law. At larger force and for all contacts realized, one expects $t = 1/3$ (microscopic exponent derived from Hertz law). A constant $t$ exponent is generally observed on 1 or 2 decades in pressure. Simple models, based on the effective medium theory or on the strongest stresses network, have been proposed to describe electrical laws [6].

Nevertheless, a warning should be given about the interpretation of electrical (or mechanical) experiments using small cylinder or particle packings. Indeed, finite size effects and wall effects may be present [8]. In the limit of small particle packing thicknesses, size effects inducing small values of the conductivity exponent are dominant [6]. For packing thicknesses comparable to cell dimensions, it has been shown that blocking resulting from friction at the walls may be important and limits the transmission of forces across the assembly because of arching effects [8–10]. In this case, the resistivity of the packing increases monotonically with the number of layers and one has to take into account an inhomogeneous distribution of pressure along the thickness of the packing [6,10].

Our goal deals with a better understanding of the compaction process of Si particles and of the possible correlation between sintered sample and corresponding compaction step. In this study, compaction process is studied from in situ resistivity measurements performed on different weights (*i.e.*: heights) of Si particles. Wall effects are evidenced in the study and the influence of the inhomogeneous distribution of pressure on the macroscopic conductivity of the packing is tentatively discussed. Comparison of the conductivity variations observed on Si sintered pellets and particle packings with various thicknesses are finally performed.

## 2 Experimental details

Si powders have been produced by grinding monocrystalline silicon samples in a planetary ball miller. Monocrystalline silicon is doped with boron and its resistivity is about 3–5 $\Omega$ cm. Container and balls are made of agatha (99% of $SiO_2$) in order to minimize impurity production. Mass ratio between silicon and balls is 4 and rotation speed is fixed at 200 cycles per minute. Under these conditions, grain sizes of Si powder are distributed in the range 5–40 $\mu$m for a milling time of 90 mn.

In order to study the effect of bed powder height on the compaction and sintering processes, different weight of Si particles (ranging from 0.02 to 1 g) are packed in a cylindrical home-made cell (see Fig. 1). The packings were formed by pouring the Si powder into the home-made cell. Packing was then subjected to mechanical vibrations in order to slightly rearrange the loose array of particles. Before starting the uniaxial compression, the force exerted on the packing is about 0.1 N which corresponds to the weight of the upper sliding piston (see Fig. 1). The internal vertical walls of the home-made cell are insulated with $Al_2O_3$ and the upper and lower walls consists in stainless steel to prevent deformation of the cell and insure good electrical contacts. The samples are placed in an MTS 810 universal testing machine and an uniaxial vertical force, ranging from 0 to 50 kN, is applied. Given the diameter of the cell (1.0 cm), the maximum applied force corresponds to a pressure of 640 MPa. Electrical resistance measurements are performed as a function of applied force with a multimeter (Keithley model 2000) which allows to measure either the voltage drop (current source mode), the current flow (voltage source mode) or the resistance (ohmeter mode) depending on the resistance range being measured. The measurements are done at increasing pressure as the force is known to be no more uniaxial on the decreasing part of the hysteresis [11]. A displacement sensor allows to measure the thickness ($e$) of the pellet during uniaxial compression. From the thickness of the pellet, one can easily calculate the conductivity of the Si pellet and its variations with applied force.

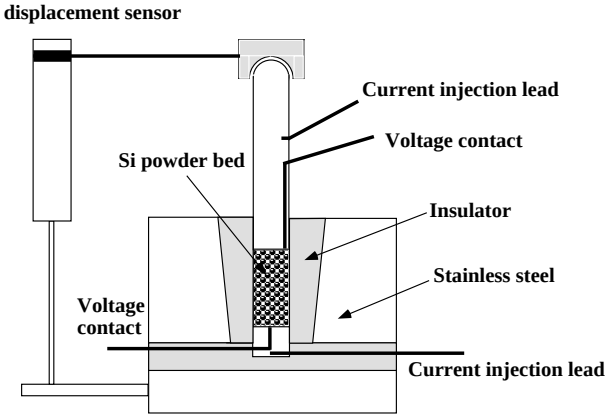


**Fig. 1.** Schematic representation of the home-made cell used for resistance measurements under uniaxial compression.

After compaction, the Si pellets have been sintered at 950 °C for 2 hours in an Ar low pressure ($10^{-1}$ hPa) in order to avoid oxidation. Scanning electron microscopy (SEM) analysis was then performed in order to check the morphology of the sintered pellets. Resistivity measurements were also performed using a four probe equipment in order to compare transport properties of the sintered samples with different thicknesses.

## 3 Results and discussion

Figure 2 shows the conductivity variations of different Si particle weights as a function of the applied force $F_0$. For a constant weight of Si powder, the macroscopic conductivity largely increases with applied force. At small applied

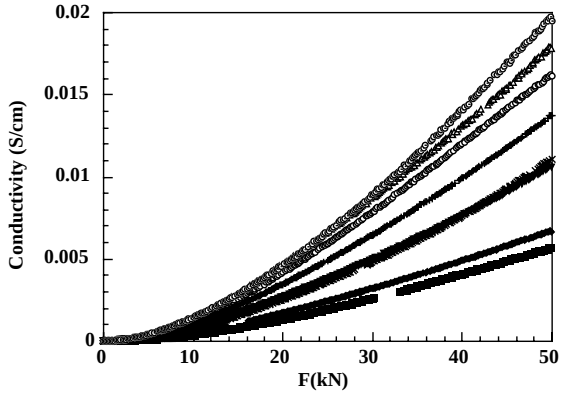


**Fig. 2.** Conductivity *vs.* force applied on different weight of Si particles. From bottom to top of the figure, Si weights are 1, 0.8, 0.5, 0.35, 0.2, 0.1, 0.05, 0.025 g.

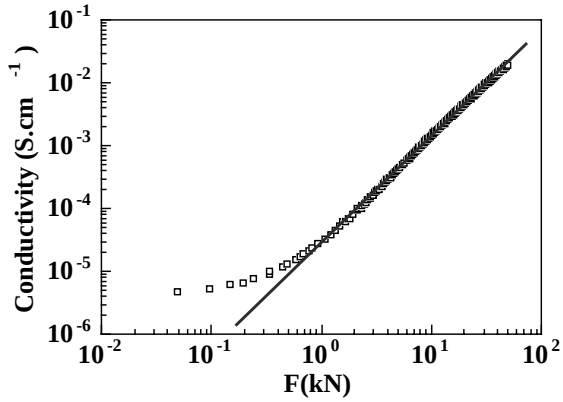


**Fig. 3.** Log-Log plot of the conductivity *vs.* force applied on 0.025 g of Si particles. In the range 2–50 kN, a power law regime with an exponent 1.7 is evidenced.

force, macroscopic conductivity likely increases due to the large increase of the density of contacts between Si particles. At larger applied force, the increase of the conductivity may result from both the contact conductance (Hertz effect) and the contact density variations. Variations of the conductivity measured on the smallest weight of Si powder (*i.e.* 0.025 g) is plotted, in log-log scale, as a function of the applied force in Figure 3. A linear variation is clearly evidenced for applied forces in the range 2–50 kN. As a consequence, macroscopic conductivity varies as a power law of the form:

$$\sigma = C_0 F^t \tag{1}$$

where the exponent $t$ is $1.70 \pm 0.02$. This result is in agreement with previous measurements performed on packing of conducting spheres ([6] and references therein) and suggests that the variations of the conductivity with applied force is dominated by the modification of the strongest stresses network.

For larger weight of Si powder (*i.e.*: for larger bed powder thicknesses), the power law is no longer valid on the same range of force. Moreover, the conductivity appears, in Figure 2, as a decreasing function of the Si powder

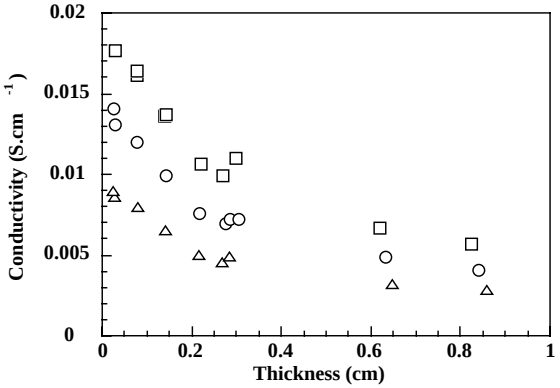


**Fig. 4.** Conductivity *vs.* thickness of the Si pellet. Open squares, open circles and black circles are respectively obtained for applied force 50, 40 and 30 kN.

weight. Such a result is clearly evidenced in Figure 4 which shows the conductivity measured at constant applied force as a function of the Si bed powder thickness. Such a behavior indicates that the resistance increases monotonically with the number of Si layers but also that the slope of the curve (the differential resistance) is an increasing function of thickness ($e$). It is characteristic of a non ohmic behavior. Such a result has been previously observed on a mixture of conducting and insulating spheres [10] and is connected with the inhomogeneous distribution of pressure in high aspect ratio container. This inhomogeneous distribution of pressure results from frictions between particles and between particles and wall-cell. Near the surface where force is applied, particles are compressed and form a structure (arch) that is leaned on the wall cell and prevent hydrostatic transmission of the force [12].

A model based on the experimental observation that a granular medium redirect vertical stress along horizontal directions has been proposed by Janssen [13] and Lord Rayleigh [14]. A generalised expression of the Jansen equation may be obtained in [15]. Thus, the force lying along the $z$ axis of the cell may be written as:

$$F(z) = F_0 \mathrm{e}^{-(2k\mu_\mathrm{s}\, z/r)} \tag{2}$$

where $F_0$ is the force applied on the top of the cell, $k$ is defined as the ratio between radial and axial pressures [13], $\mu_\mathrm{s}$ is the friction coefficient between particle and wall-cell, $r$ is the cell radius and $z$ the distance from the top of the cell. Such a variation of the force with packing thickness has also been experimentally observed on copper particles [16].

As the conductivity is an increasing function of the applied force (*cf.* Eq. (1)), the local conductivity of a layer of thickness d$z$ must decrease with the distance ($z$) from the top of the cell. Under this condition, the array of Si particles may be viewed as series resistors along the $z$ axis. One can calculate the equivalent macroscopic conductivity of such a system with total thickness $e$:

$$\frac{\sigma(e)}{C_0 (F_0)^t} = \frac{(2k\mu_\mathrm{s} t)e}{r\left(\mathrm{e}^{+(2k\mu_\mathrm{s} t\, e/r)} - 1\right)} \tag{3}$$

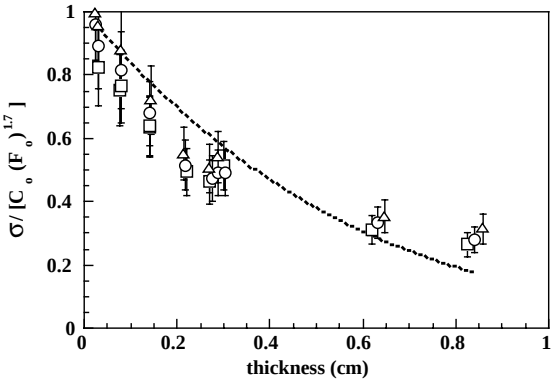


**Fig. 5.** Normalized conductivity $\sigma/[C_0(F_0)^t]$ obtained at different applied force (50, 40 and 30 kN) *vs.* Si thickness. Plot evidences a single behavior whatever is the applied force. Full line is a fit of equation (3) (see text for details).

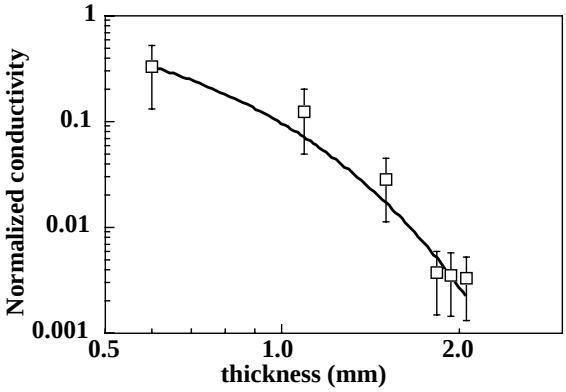


**Fig. 6.** Normalized conductivity (*i.e.* Si sintered sample conductivity over the initial Si wafer conductivity) *vs.* Si sintered pellet thickness. Full line is a fit of equation (4) (see text for details).

where $\frac{\sigma(e)}{C_0(F_0)^t}$ is the normalized conductivity. Such an equation is qualitatively equivalent to the one experimentally observed in [10].

The normalized conductivity, calculated for different applied forces, is shown in Figure 5 as a function of the Si pellet thickness. Full line corresponds to a fit of equation (3) with a single adjustable parameter ($\frac{2k\mu_s t}{r}$). All data shown in Figure 5 lie on a single curve whatever is the applied force in the range 30–50 kN.

Given the simplified expression of the force variations (Eq. (2)), the agreement between experimental and fitted results is quite reasonable. Moreover, the value $k\mu_s = 0.48 \pm 0.01$ used for the fit is in compatible agreement with the known range of values (0.3–0.7) and (0.4–1.2) for $k$ and $\mu_s$, respectively.

In a next step, Si pellets were sintered at 950 °C for 2 hours and resistivity measurements were performed at room temperature as a function of the sintered pellet thickness. Normalized conductivity of the sintered Si pellets (*i.e.* ratio of sintered sample over Si wafer conductivities) is plotted in Figure 6 as a function of the sample thickness. As in the compaction process, the conductivity is a decreasing function of the pellet thickness. This behavior is thought to result from the compacity gradient introduced during the compression step. If so, one can write, in a first approximation and as done in previous section, that local conductivity exponentially decreases with pellet thickness. Thus, the conductivity variation with Si sintered pellet thicknesses is given by:

$$\sigma(e) \propto \frac{e}{\ell_c \left(e^{+(e/\ell_c)} - 1\right)} \qquad (4)$$

which is similar to equation (3) and where $\ell_c$ corresponds to a characteristic length below which the conductivity gradient becomes small. Comparison between experimental and calculated conductivities are shown in Figure 6. Although the experimental errors in conductivity measurements are quite large, it can be noticed that equation (4) may account for the results. As a consequence, the variation of the conductivity with Si sintered pellet thicknesses likely finds its origin in the compacity gradient introduced during the initial compaction step. The characteristic length ($\ell_c$), deduced from the fit, is $(250 \pm 20)$ $\mu$m.

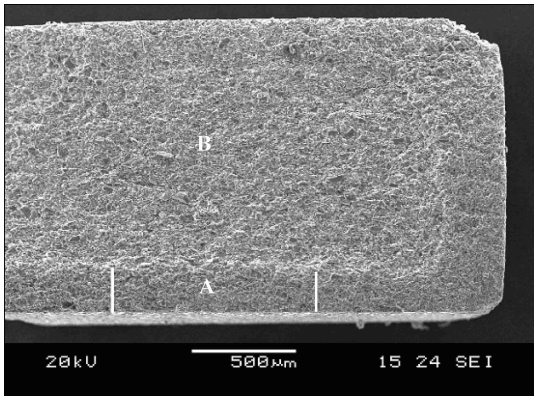


**Fig. 7.** Scanning electron micrograph obtained on the cross section of a Si sintered sample. Vertical axis corresponds to the direction of the uniaxial compression.

Scanning electron microscopy was performed on the cross section of a cut and polished sample in order to estimate the compacity variation along the sample thickness. Figure 7 shows such a scanning electron micrograph of a sintered pellet whose initial thickness was 2 mm. It is evidenced, in the micrograph, that morphology is different at the bottom (region A) and in the bulk (region B) of the sample. Figure 8 shows scanning electron micrographs obtained in A and B regions. In region A, a large number of necks between Si particles are observed whereas compacity of the B region appears lower. These observations are in qualitative agreement with the existence of a conductivity variation along the sample thickness. Indeed, the large number of necks between Si particles increases the local conductivity of the A region. As estimated from Figure 7, the high compacity region extends over $(220 \pm 30)$ $\mu$m. One can notice that this result is in quantitative agreement with the characteristic length ($\ell_c$) extracted from the fit of equation (4). Thus, the characteristic length below which the conductivity can be considered as slowly

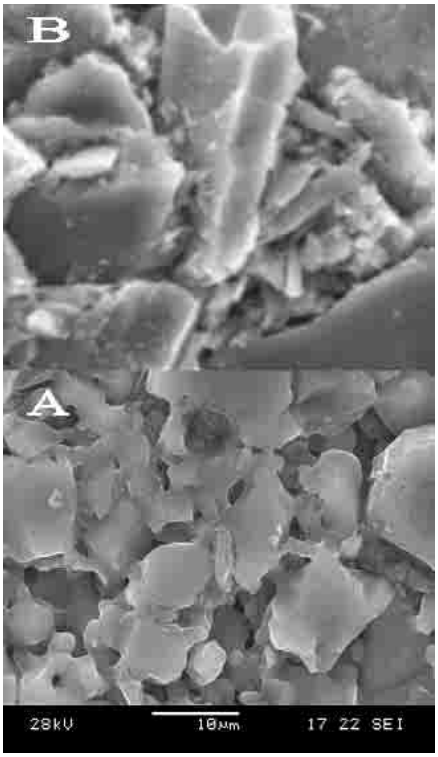


**Fig. 8.** Scanning electron micrographs obtained on A and B regions defined in Figure 7.

varying seems to be related to the extend of a high compacity region. These results suggest that the final properties of the sintered samples strongly depends on the initial compacity and on its distribution within the sample. At this stage, it may be interesting to increase sintering time and/or temperature in order to correlate kinetic effects and compression process effects. Indeed, the extend of the high compacity region, and thus the characteristic length evidenced in transport measurements, may increase with sintering time and temperature.

## 4 Conclusion

In summary, resistivity measurements have been performed on Si powder beds of different thicknesses while varying uniaxial pressure. It is shown that the resistivity variations may be understood by taking into account the distribution of pressure along the sample thickness. Although the expression used to account for the pressure distribution appears very simple, our experimental and calculated data are in reasonable agreement. It is shown that a similar conductivity gradient likely exists in sintered samples. Such a conductivity gradient very likely finds its origin in the variation of the compacity along the sintered sample thickness. Such a variation of the compacity comes from the initial compaction process. Thus, the final resistivity of the sintered samples largely depends on the compaction conditions. This result suggests that modelisations of the sintered process have to take into account the compacity gradients resulting from the compaction process.

This work was partly supported by the ADEME-CNRS french ECODEV program actions for renewable energies ARC polycrystalline silicon layers, contract I.3.07.

## References

1. E. Béré, A. Straboni, P. Grosbras, D. Mencaraglia, C. Bodin, *E-MRS Spring meeting, Strasbourg (France), June 5–8, 2001.*
2. T. Travers, M. Ammi, D. Bideau, A. Gervois, J.C. Messager, J.P. Troadec, Europhys. Lett. **4**, 329 (1987).
3. J.P. Trodec, D. Bideau, Onde Électr. **71**, 30 (1991).
4. D. Stauffer, H.J. Herrmann, S. Roux, J. Phys. France **48**, 347 (1987).
5. H.J. Herrmann, D. Stauffer, S. Roux, Europhys. Lett. **3**, 265 (1987).
6. M. Ammi, T. Travers, D. Bideau, A. Gervois, J.C. Messager, J.P. Troadec, J. Phys. France **49**, 221 (1988).
7. K.J. Euler, J. Power Sources **3**, 117 (1978).
8. E. Guyon, S. Roux, A. Hansen, D. Bideau, J.P. Troadec, H. Crapo, Rep. Prog. Phys. **53**, 373 (1990).
9. P. Dantu, Ann. Ponts et Chaussées **IV** (1967).
10. G. Giraud, J.P. Clerc, E. Guyon, Powder Technol. **35**, 107 (1983).
11. J. Feda in *Mechanics of particulate materials* (Elsevier, Amsterdam, 1982).
12. H. Ottavi, J. Clerc, G. Giraud, J. Roussenq, E. Guyon, C.D. Mitescu, J. Phys. C **11**, 1311 (1978).
13. H.A. Janssen, Z. Vereins Deutsch Ing. **39**, 1045 (1895).
14. O.M. Lord Rayleigh, Phil. Mag. S6 **11**, 61 (1906).
15. J. Duran, *Introduction à la physique des milieux granulaires* (Eyrolles Sciences, Paris, 1997), p. 88.
16. R.A. Thompson, Ceramic Bull. **60**, 237 (1981).